Novel Spectral Decay Dynamics of Hot Excitons in PbSe Nanocrystals: A Tunable Femtosecond Pump–Hyperspectral Probe Study

ARTICLE *in* THE JOURNAL OF PHYSICAL CHEMISTRY C · NOVEMBER 2013

Impact Factor: 4.77 · DOI: 10.1021/jp409530z

6 AUTHORS, INCLUDING:

Chunfan Yang
Hebrew University of Jerusalem
6 PUBLICATIONS **7** CITATIONS
SEE PROFILE

Diana Yanover
Technion - Israel Institute of Technology
17 PUBLICATIONS **80** CITATIONS
SEE PROFILE

Hanan Sachs
Hebrew University of Jerusalem
4 PUBLICATIONS **30** CITATIONS
SEE PROFILE

THE JOURNAL OF PHYSICAL CHEMISTRY C

Article

pubs.acs.org/JPCC

Novel Spectral Decay Dynamics of Hot Excitons in PbSe Nanocrystals: A Tunable Femtosecond Pump–Hyperspectral Probe Study

Itay Gdor,[†] Chunfan Yang,[†] Diana Yanover,[‡] Hanan Sachs,[†] Efrat Lifshitz,[‡] and Sanford Ruhman*[,†]

[†]Institute of Chemistry, The Hebrew University, Jerusalem 91904, Israel

[‡]Department of Chemistry and Solid State Institute, Technion, Haifa 32000, Israel

Supporting Information

ABSTRACT: Ultrafast exciton cooling in highly monodisperse PbSe nanocrystals is followed with tunable pump–hyperspectral near-IR probe spectroscopy. Unexpected kinetic and spectral correlations between induced bleach and absorption features are revealed, which are incompatible with standard models for excited nanocrystal absorption. Interband optical excitation immediately generates a sharp bleach feature near the $1S_h1S_e$ transition which is unchanged during exciton thermalization, while pumping well above the band edge induces an intense absorption at frequencies just below the band edge which decays concurrently with a buildup of renewed absorbance at the $1P_h1P_e$ peak during exciton cooling. Transient spectra of hot single and double excitons are nearly indistinguishable, arguing against the controversial involvement of Auger cooling in the rapid dissipation of excess energy in excited PbSe QDs. Finally, quantitative signal analysis shows no signs of multiexciton generation up to photon energies four times the sample band gap.

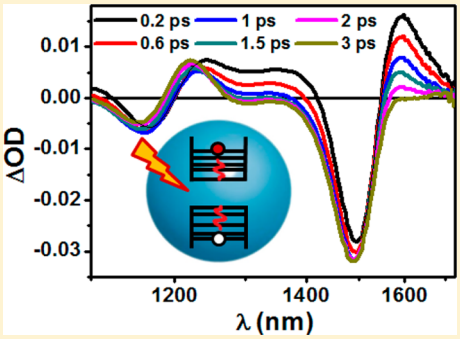

INTRODUCTION

Excitation of bulk semiconductors with photon energies in excess of the band edge leads to a rapid phonon-assisted intraband relaxation of both electron and hole. In semiconductor quantum dots (QDs) the size-induced quantum confinement gives rise to a discrete electronic density of states close to the band edge.[1] It was postulated that this sparse energy spectrum would significantly slow intraband relaxation due to the mismatch of energy spacing in the phonon and electronic state manifolds. This so-called "phonon-bottleneck",[2] was of fundamental interest and also deemed practically significant since it might open the way for boosting the efficiency of solar devices.[3,4]

Experiments show that although semiconductor QDs typically have spacing between electronic energy bands which can reach hundreds of meV, far exceeding phonon energies,[5] fast relaxation times (femtosecond to picosecond) were observed in various semiconductor QDs.[6,7] To explain the absence of the expected bottleneck, fast electron–hole energy transfer or "Auger cooling"[8−12] was postulated. In this mechanism, the excess energy of the electron is transferred to a hole, which later loses it rapidly by phonon emission due to the often denser valence-band level spacing. In PbSe, however, electrons and holes have similar effective masses, predicting symmetry in level spacing between the conduction and valence bands[13,14] and irrelevance of Auger cooling in breaking such a phonon bottleneck. Contrary to these expectations, measurements show that carrier cooling dynamics in PbSe QDs are fast and occur on subpicosecond to picosecond time scales as in other semiconductor nanodots.[15,16]

To explain this inconsistency Schaller et al.[17] have suggested a mechanism involving efficient multiphonon emission triggered by nonadiabatic electron–phonon interactions. Another possible explanation for the rapid decay time is found in pseudopotential calculations done by An et al.[18,19] which show that hole energy levels are more densely spaced than predicted by less rigorous models due to coupling between multiple valence band maxima, paving the way for efficient Auger cooling after all.

Ultrafast transient absorption (TA) spectra, which serve to measure exciton dynamics in QD samples, have been interpreted with two main effects: state filling and biexciton interactions.[20,21] The former derives from the Pauli exclusion principle where filling of electronic states leads to blocking of the corresponding optical transitions, while biexciton Coulomb interactions lead to modifications in level energies and to frequency shifts in related optical transitions. In the context of TA spectroscopy, biexciton shifts involve interactions of e–h pairs excited by the pump pulse with an additional exciton generated by the probe.

Assuming that this picture is correct, excitation high above the band edge should not alter the occupancy of the HOMO or LUMO, and immediately after excitation any changes in

Received: September 24, 2013
Revised: November 20, 2013
Published: November 20, 2013

absorption at the band edge should stem only from biexciton shifts. For attractive biexciton interaction the resulting variations in energies will induce enhanced absorption on the red side of the band gap (marked as A1[6]) and a negative signal near the $1S_e1S_h$ absorption peak. Pioneering experiments focusing mainly on CdSe QDs showed that following a rapid initial appearance the band edge bleach signal continues to rise gradually over a period of several picoseconds.[16,21,22] The rise component was attributed to the cooling from the excited $1P_e1P_h$ state to the band edge and a switch from biexciton shifting to state filling.

Making allowances for the 4-fold difference in band edge state degeneracy, TA experiments on PbSe QDs have also been interpreted using these same mechanisms, again detecting a delayed rise of the band edge bleach as hot excitons cool.[16] In a previous work,[23] however, we found several fundamental inconsistencies between the picture presented above and high time resolution TA experiments with PbSe QDs. The objective of this study is to quantify and analyze those differences to understand the cooling dynamics of "hot" single- and multiexcitons in colloidal PbSe QDs. The highly monodisperse samples employed here have facilitated selective pumping and probing in particular optical transitions, which is essential for deciphering the spectral evolution associated with hot exciton cooling.[24,25] The broadband hyperspectral probing apparatus used offers detailed spectral characterization of the sample during exciton cooling,[23,26] demonstrating that the accepted mechanisms underlying TA of QDs are insufficient for explaining all our observations. As outlined below, the transient spectra recorded are also at odds with recent theoretical predictions concerning the effective cooling mechanisms of hot excitons in PbSe QDs.

EXPERIMENTAL METHODS

Sample Preparation. The reaction mixture, consisting of 0.4 mmol of PbO, 1.2 mmol of oleic acid (OA), and hexadecane (HDC) (the total mass of the reaction mixture was adjusted to 8 g by adjustment of the amount of HDC), was heated to 100 °C under vacuum for 1 h. Then, under a nitrogen atmosphere, the temperature was adjusted to 80 °C. The selenium precursor solution, containing 0.8 mL of 1 M trioctylphosphine selenide (TOPSe) solution, 0.15 g of diphenylphosphine (DPP), and HDC (total volume of injection solution was 4 mL), was then injected into the reaction mixture. The temperature was reduced to the growth temperature of 70 °C. To quench the reaction and to perform the first precipitation, the flask was opened at standard atmosphere, and the reaction mixture was poured into a mixture of ethanol, acetonitrile, and toluene (volume ratio of 3:3:4). The QDs were separated by centrifugation. For the second precipitation, the test tube was transferred to a nitrogen-filled glovebox where the test tube was opened, and the supernatant was removed. The precipitate was then dissolved in hexane, and the 2-fold volume (relative to the hexane) of acetonitrile was added. A two-phase system formed, while the QDs were present in the hexane phase. The 4-fold volume (relative to the hexane) of ethanol was subsequently added dropwise, which caused the disappearance of the second phase and a precipitation of the QDs. The precipitate was separated again by centrifugation. Then, the supernatant was removed, while the precipitate was dried under a nitrogen atmosphere and finally dissolved in hexane under a nitrogen atmosphere. Transmission electron microscopy (TEM) of the synthesized QDs is presented in Figure 1.

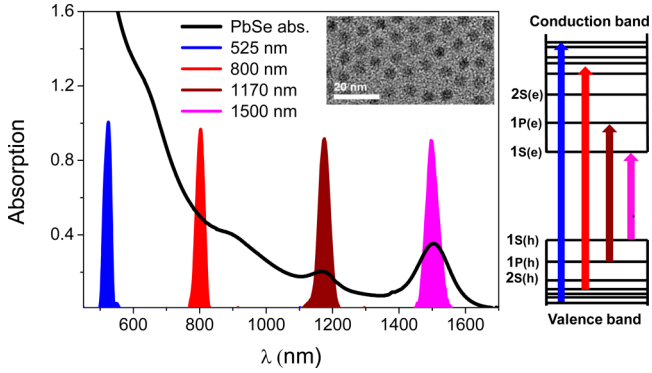

Figure 1. Absorption spectra and TEM of the PbSe QDs, along with intensity spectra of the four excitation pulses used. On the right is a schematic energy diagram based on ref 18.

Pump–Probe Experiments. All samples were handled in oxygen-free environments and irradiated in airtight 1 mm path length optical glass cuvettes at room temperature. The laser system and methods of measurement have been described in detail elsewhere.[27] A few microjoules of the 30 fs amplified output from a homemade multipass titanium sapphire system served to generate a white light continuum probe by focusing in 3 mm of sapphire. The continuum pulses were collimated and refocused into the sample using reflective optics. Another portion of the amplified fundamental was used to generate pump pulses, either directly at ~800 nm or by pumping a TOPAS (Light Conversion) to produce ~40 fs pump pulses centered at 1500, 1170, and 525 nm, and the intensity spectra are shown in Figure 1 as well. Kerr scans on glass provided the probes' wavelength-dependent group delay and indicated a pump–probe cross-correlation of sub 100 fs throughout the probed range. After the sample, the probe pulses were collected into an InGaAs PD array spectrometer (BTC262E, BWTek) alternating with and without sample pumping. Subtraction of these produced the time-dependent difference spectra displayed below, which have been corrected for the measured probe group delay. All reported experiments were run on static samples after test runs on translating cells were shown to be identical to stationary ones. Signal decay kinetics, particularly at low pump fluences, provide additional indications that no photocharging effects were present.

RESULTS

1. Transient Absorption. Figure 1 presents the absorption spectra of the PbSe QD sample, along with the intensity spectra of the four pump pulses employed. The two lower-frequency pulses were tuned on resonance with the sharp transitions at 1170 and 1500 nm. For investigating relaxation of even more energetic excitons, the laser fundamental at 800 nm and doubled OPA pulses at 525 nm were utilized as well. As seen in the schematic energy diagram on the right of Figure 1, the prominent band edge absorption feature, in our case centered at 1500 nm, is attributed to a transition with both the electron and hole having a 1S envelope function ($1S_h1S_e$, abbreviated in what follows as the 1S band). The second absorption is assigned to a transition with both electron and hole having a 1P envelope function ($1P_h1P_e$, abbreviated accordingly as 1P).[28,29]

dx.doi.org/10.1021/jp409530z | J. Phys. Chem. C 2013, 117, 26342–26350

This assignment is not unanimously accepted and has been attributed by others to a transition to the forbidden $1S_h1P_e$/$1P_h1S_e$ states.[30,16] At shorter wavelengths, only faint additional spectral features are discernible around 900 nm, superimposed on a steeply rising absorptive background.

The initial 3 ps of spectral evolution following excitation at t = 0 of these PbSe QDs with the depicted pump pulses is presented in Figure 2 as sequences of transient difference

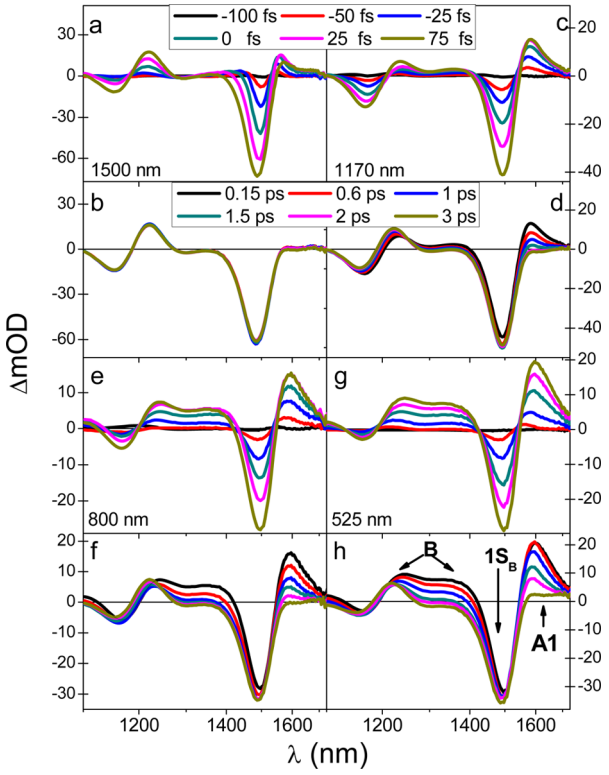

Figure 2. Transient difference spectra presented as temporal cuts at the designated pump−probe delays, after excitation at 1500 nm (a,b), 1170 nm (c,d), 800 nm (e,f), and 525 nm (g,h). Early designated times pertain to panels a, c, e, and g, while later delays apply to all other panels.

absorption spectra at delays indicated in the figure legend. Delays in the ranges 0−75 fs and 0.15−3 ps are presented above and below, respectively, for progressively higher pump frequencies. Pump photon fluxes in both were controlled to deposit ∼1 exciton per QD on average at the front surface of the sample ($\eta \equiv \sigma J \approx 1$), which had an OD of 0.5 at 1500 nm.

At all four excitation wavelengths, photon absorption leads to an immediate buildup of an intense bleach feature centered near the 1S absorption peak. Near the 1P transition a more intricate spectral change is observed. Above band edge excitation gives rise immediately to a superposition of bleach and red shift which converges within picoseconds to a biexciton shifting band shape known to characterize the difference spectrum after cooling. Along with these localized spectral changes, a broad absorption which extends to wavelengths above that of the band edge also appears promptly when exciting above the band edge, a phenomenon which has been reported for CdSe QDs.[25,31] The amplitude and the spectral range of this early absorption are enhanced with the increase of exciting photon energy, and the picosecond decay of this broad positive TA band is a major component of spectral evolution during cooling.[23]

This decay in absorption however does not take place with the same rate throughout the probed range. As seen most clearly for the shorter pump wavelengths, a prompt broad induced absorption spanning the 1500 and 1170 nm range decays faster than the sharp induced absorption peak just below the 1S band, a point that will be elaborated upon below. After this initial ∼3 ps of delay, the signal converges to that observed immediately following excitation at 1500 nm—an excess transmission feature at the band edge and a peak shift signature associated with the second absorption band at ∼1170 nm.[29] In particular the spectrally distinct sharp band edge bleach remains essentially constant throughout the process of cooling portrayed in the lower panels of Figure 2. To facilitate further discussion of this data we will define abbreviations for the main features observed in TA, as designated in Figure 2: A1 for the below band edge enhanced absorption, "$1S_B$" for the bleach at 1500 nm, and band B referring to the continuous absorption extending between the 1S and 1P bands.

2. Measures of Exciton Cooling Dynamics. To facilitate interpretation, the hyperspectral data were processed in two fashions. One was the calculation of difference dipole strengths, or band integrals, over the full probing range of 1100−1730 nm according to the following equation $\Delta D(t) \equiv \int((\Delta\mathrm{OD}(\nu,t))/\nu)\mathrm{d}\nu$ resulting in a single value for each time delay.[32] The significance of this measure will be explained shortly. The second was to calculate finite time difference spectra: $\Delta\Delta\mathrm{OD}(\lambda,t,\Delta t) \equiv \Delta\mathrm{OD}(\lambda,t + (\Delta t/2)) - \Delta OD(\lambda,t - (\Delta t/$

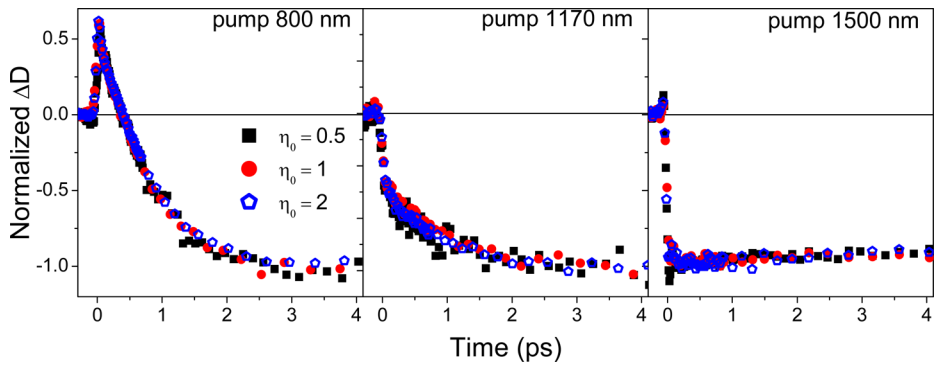

Figure 3. Normalized band integrals over full difference spectrum ($\int((\Delta\mathrm{OD}(\nu,t))/\nu)\mathrm{d}\nu$) vs delay ($t$) for pumping at 800, 1170, and 1500 nm with three excitation intensities adjusted to produce the designated values of η_0, the average excitons per quantum dot at the front surface of the sample cell.

dx.doi.org/10.1021/jp409530z | J. Phys. Chem. C 2013, 117, 26342−26350

2)), where $\Delta OD(\lambda,t)$ represents transient spectra like those presented in Figure 2, at delays differing by a specific margin Δt. The rationale of this latter approach was to generate effective derivatives of the difference spectra with delay time. These serve to indicate how the difference absorption spectrum varies with time, without interference from the intense and long-lived bleach and peak-shift features which appear to dominate the difference spectra during much of the cooling process.

2.1. Difference Dipole Strength. The state-filling and biexciton shift mechanisms invoked for rationalizing interband pump−probe data in nanocrystals should either reduce or not influence the sample dipole strength, respectively. Assuming interaction energies to be in the meV range, neither of these mechanisms should cause a significant increase in ΔD. Within the Condon approximation it is the dipole strength which should remain unchanged despite spectral shifting of the various contributions to the difference spectrum. Accordingly the time dependence of ΔD tests the interplay between the various mechanisms which alter absorption during cooling. Results of this analysis are presented in Figure 3 for the three longest excitation wavelengths, at a series of pump fluences.

Tuning the excitation wavelength leads to a very different time evolution of ΔD. After 800 nm excitation the difference dipole strength starts out positive, i.e., reflects a net *increased absorption*, which reverts to net bleach within hundreds of femtoseconds. This is true for 525 nm excitation as well, differing only in a slower transition from positive to negative ΔD.[23] It later becomes gradually more negative over the ∼3 ps period of cooling. In contrast, excitation into the 1P band at 1170 nm causes an immediate reduction in the integrated dipole strength, which then roughly doubles in absolute value over the course of cooling. Band edge excitation causes instantaneous reduction in the band integral with no variation thereafter. At all three pump wavelengths, variations in fluence which alter the distribution of exciton number states appear not to influence the time dependence of the normalized ΔD.

ΔD dynamics for the two longer pump wavelengths are qualitatively compatible with spectral changes reflecting state filling and biexciton shifts alone. As expected, no increase in dipole strength is observed in either. Exciting at the band edge also leads to no evolution of ΔD after the initial abrupt fall, in accordance with direct generation of ″cold″ excitons. The prompt decrease of ΔD when pumping at 1170 might reflect direct state filling in the 1P state, and the gradual decrease during cooling reflects decay to the band edge where state filling in the 1S states blocks an even stronger transition. This compatibility ends when exciting higher in the absorption continuum. Contrary to expectations, the energetic photons create hot excitons whose dipole strength in the probed range increases significantly. Possible mechanisms giving rise to this additional dipole strength will be discussed below.

2.2. Finite Time Difference Spectra. For understanding the unexpected initial positive ΔD when exciting with large $h\nu$, attention must be directed to the fine spectral details of the TA spectra. This is aided by reviewing plots of finite time difference spectra, designated as $\Delta\Delta OD(\lambda,t,\Delta t)$. Before presenting these, Figure 4 exhibits the limits of signal evolution during cooling for all above band-edge pump wavelengths. Panel A presents $\Delta OD(0)$, the instantaneous TA signals, normalized to the same $1S_B$. These spectra are obtained from the TA data by deconvolution from the instrument response and subtraction of contributions from coherent artifacts. They approximate

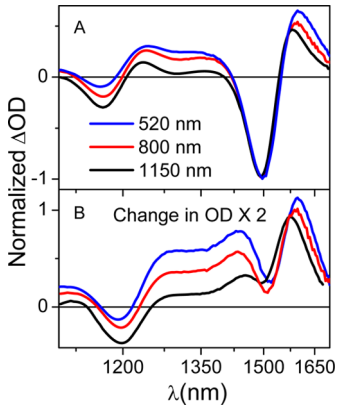

Figure 4. Panel A: immediately rising TA signal at the three designated pump wavelengths. Panel B: The change in TA over the course of cooling (multiplied by 2).

initial changes in absorption in the nascent sample before the onset of cooling. Panel B presents $\Delta OD(3\ ps) - \Delta OD(0)$, the total change in sample absorption over the course of exciton cooling. Noting that the changes in panel B have been multiplied by 2 demonstrates the utility of $\Delta\Delta OD(\lambda,t,\Delta t)$ as a measure of cooling spectral evolution which avoids masking from the prominent features in $\Delta OD(0)$.

Overlays of $\Delta\Delta OD(\lambda,t,\Delta t)$ spectral sequences are presented in Figure 5, calculated for a period of evolution (Δt) of 300 fs.

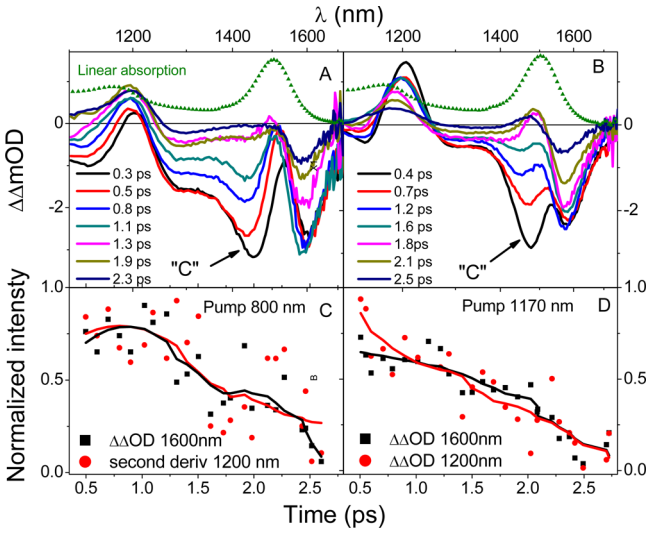

Figure 5. Series of finite time difference spectra obtained by subtracting the ΔOD data over the interval of 300 fs at times designated in the legend after 800 nm (A) and 1170 nm (B) excitation. Panel C and D present the time dependence of ΔΔOD at 1200 and 1600 nm after 800 and 1170 nm excitation, respectively.

Starting with the highest photon energy of ∼1.5 eV (800 nm), on the shortest time scales, intricately structured ΔΔODs are revealed. In accordance with the band integral results, across the probed spectral range the ΔΔOD is in general negative, as expected for a net reduction in difference dipole strength. This trend is however not evenly distributed over the probed spectrum. A localized peak at 1600 nm (A1) dominates the red edge of the finite difference spectra throughout the cooling process. Adjacent to this is an equally sharp cleft extending all the way to zero and coinciding with the 1S peak. Further to the

dx.doi.org/10.1021/jp409530z | J. Phys. Chem. C 2013, 117, 26342−26350

blue, negative ΔΔOD builds up sharply exhibiting a peak at 1450 nm and tailing all the way to the high frequency edge of our detection. Finally, at the position of the 1P transition, a positive ΔΔOD peak is superimposed on the tailing edge of the broad negative background.

The delay dependence of ΔΔOD spectra is nonuniform, suggesting that it is made up of several distinct contributions. The broad negative background extending from 1450 to 1100 nm fades within a fraction of a picosecond, with the sharp peak at its red edge disappearing fastest of all. Two narrow spectral peaks remain nearly constant in the ΔΔOD spectra during the course of this decay, the A1 band and a somewhat weaker positive peak near the 1P transition which will be coined ″A2″. These two features are present from the earliest decay times but outlive the fast fading of the broad negative feature and later decay in sync over several picoseconds. Since ΔΔOD presents a derivative with time of the difference spectra, the initial constancy in amplitude of both indicates a linear decay over this period. It is noteworthy that during its decay the A1 peak has no adjacent oppositely signed band to the blue which should show up if this decay is due only to decay of a spectral shift feature.

To verify that both A1 and A2 bands decay with similar kinetics, measures were devised to isolate them from the rapidly decaying absorptive background. The A1 peak in the red is sufficiently isolated for its amplitude to be assessed directly in the TA data. As for that centered near 1200 nm, a second derivative was performed on the finite time difference spectra for its isolation after 800 nm excitation. When pumping in the 1P band the B induced absorption is sufficiently shallow to allow both amplitudes to be obtained directly from the TA signals. As can be seen in Figure 5C which presents the normalized amplitudes of the two measures, the dynamics fit one another perfectly within the experimental uncertainty, indicating that their decay reflects a single relaxation process. Similar analysis of the 1170 nm excitation data is shown in panel B of Figure 4. The broad background absorption is barely observable in this case, while the intense 1450 nm peak as well as A1/A2 are clearly observable initially, later decaying on very different time scales.

2.3. Kinetic Analysis. Evidence for distinct contributions of hot excitons to TA is obvious both from the kinetics and from pump wavelength dependence of the spectra in Figures 2, 4, and 5. The broad B band is virtually absent when exciting into the 1P transition and grows in intensity continuously as the excitation photon energy increases all the way to 520 nm—the shortest pump wavelength we have used. In contrast, the extremely short-lived 1450 nm peak, which will be coined band ″C″ (see Figure 5), is present for all above band edge excitations. Ideally, separation of distinct bands in transient spectra should be possible by global kinetic analysis. This was attempted here, but due to the significant overlap of the bands and the complexity of the decay patterns, this approach was unfruitful.

As an alternative, measures were defined to characterize the decay kinetics of the spectral features described above. Time-dependent amplitudes of the spectrally isolated A1 band were obtained directly from TA signals and in light of the lower panels in Figure 5 used to represent kinetics of the A2 band as well. B band amplitudes were obtained from the TA signal at the representative wavelength of 1320 nm which is sufficiently removed from adjacent C and A2 features. C band amplitudes were estimated as follows: ΔOD(“C”) ≈ ΔOD(1450 nm) − ΔOD(1320 nm), 1450 nm being the peak of “C” and 1320 nm as stated above estimating the B band background. Results of this analysis are presented in Figure 6 which depicts the normalized time evolution of the peak amplitudes of all three spectral features, A1/A2, C, and B.

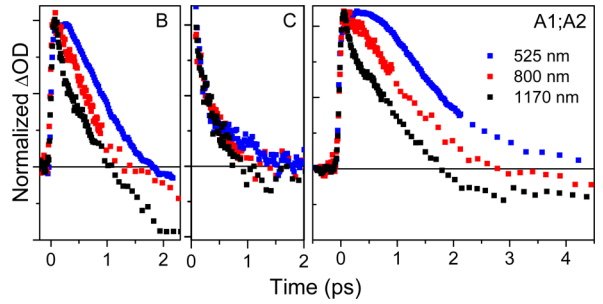

Figure 6. Decay kinetics of the B, C, and A1,2 spectral bands in the TA signals. See text for details.

The three panels of Figure 6 illustrate the kinetic distinctness of the represented bands. The C band not only decays most rapidly but also does so independently of the pump wavelength. Fitting these decays to a single exponential function leads to a lifetime of ∼350 ± 30 fs. Band B, the broad intermediate-induced absorption, is both longer lived and unlike the C feature depends strongly in both amplitude and kinetics on pump photon energy. The B amplitude decays rapidly and directly upon 1170 nm excitation. Tuning the pumping wavelength to the blue leads to an induction time during which the band amplitude is nearly constant.

This induction time grows with the pump photon energy, approaching 400 fs for 525 nm pump pulses. Following this induction time the B band amplitude decays with the same exponential time constant regardless of the pump frequency and is complete within 2 ps. A similar situation exists for the A1; A2 pair. These bands also exhibit pump photon energy dependent induction times followed by identical exponential decay kinetics. Here the induction time difference between 1170 and 525 nm excitation reaches nearly 1 ps. The amplitude of this component is however less dependent on the excitation wavelength, and for all three pump frequencies decay of these matched bands is completed on the 3 ps time scale. Results of both amplitudes and decay times of these bands are summarized in Table 1. Since the decay dynamics are markedly nonexponential, they are described with two parameters, a half-life which defines the decay time to half the original amplitude and an exponential lifetime τ which optimally fits the trailing edge of the decay.

3. Single vs Multiexcitons. *3.1. Cooling.* To this point, biexciton effects on cooling dynamics have not been explicitly addressed. It was touched upon indirectly in Figure 3 which shows that decay dynamics of the difference dipole strengths are independent of pump fluence and accordingly to the initial distribution of exciton occupation numbers. However, this can be tested more directly by separating single and multiexciton contributions to transient spectra of excited NCs. To achieve this, experiments were run with low and high fluences producing η = 0.3 and η = 2 at the front surface of the sample cell, the former leading to negligible and the latter to a very significant multiexciton population (MX). This is borne out by measurements of band edge bleach decay kinetics during Auger recombination, as presented in Figure S1 in the Supporting

dx.doi.org/10.1021/jp409530z | J. Phys. Chem. C 2013, 117, 26342−26350

Table 1. Normalized Amplitudes and Decay Kinetics of the Major Cooling Spectral Features for above Band-Edge Excitation Wavelengths

	A1/A2			C			B		
λ_{PUMP} (nm)	1150	800	500	1150	800	500	1150	800	500
$t_{(1/2)}$ (fs)	850	1300	1650	290	300	270	650	700	1050
normalized amplitude	0.49	0.53	0.55	0.15	0.14	0.12	0.05	0.2	0.27
trailing edge lifetime (fs)	1150 ± 50	1200 ± 30	1170 ± 30	340 ± 20	360 ± 10	370 ± 20	930 ± 20	825 ± 10	850 ± 10

Information. Isolation of MX transient difference spectra required an estimate of the initial distribution of exciton occupation. For known photon-fluxes, the distribution of exciton number states follows the Poisson statistics, dictated by the QD unchanging cross section for absorption at 800 nm with absorption of several photons. Including the effects of a finite sample OD on the pump flux, the distribution of exciton number states is[23]

$$\rho_N = \frac{1}{\sigma}\int_{\eta_0}^{\eta_\infty} \frac{e^{-\eta}\eta^{(N-1)}}{N!}\mathrm{d}\eta$$

where $\eta = \sigma J$ and ρ_N is the density per unit area of the N exciton state ($|N\rangle$). Using this equation the correct difference spectral density due to single excitons was calculated and subtracted from the high fluence data, producing transient spectra exclusively from multiexcitons. The fluence employed was selected so that biexcitons were by far the most probable MX state. This is important for ensuring a defacto separation of time scales between Auger recombination and exciton cooling.

The resulting spectra are presented in Figure 7 for excitation at 800 nm. The spectra of the single and multiexcitons during the cooling process are presented on the left column 300 and 800 fs after excitation. Spectral cuts at 1300 and 1600 nm which display the dynamics of features associated exclusively with hot excitons, single or multiple, are depicted on the right. The match between the spectra is nearly perfect, apart from minor shifts around the band edge bleach. Moreover, the time traces evolve identically except at very early times—sub 200 fs—a difference attributed to nonlinear wave-mixing artifacts. This perfect match in the spectral evolution during cooling of single and multiexcitons indicates that biexciton interactions have no measurable effect on the course of excess energy dissipation following above band gap excitation in PbSe QDs.

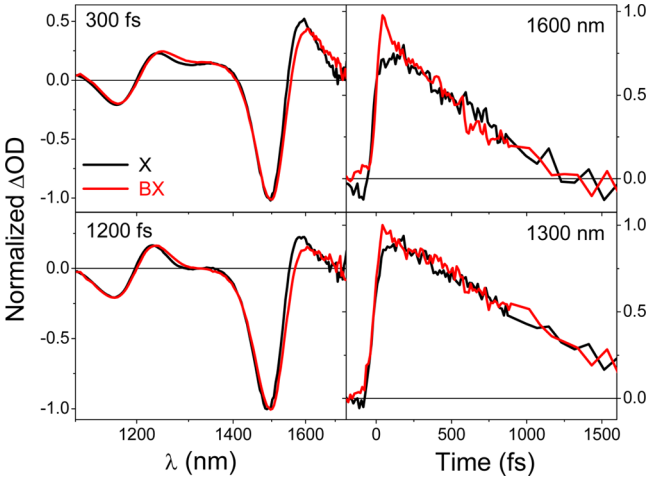

Figure 7. Comparison of single- and biexciton transient spectra after 800 nm excitation. Left: transient difference spectra at the designated pump−probe delays. Right: decay kinetics of TA at 1600 and 1300 nm.

3.2. Occurance of MEG. The claim that multiexciton generation (MEG) efficiently competes with phonon-assisted exciton cooling in QDs has attracted broad interest and generated numerous supportive observations.[33−39] In previous publications from the Ruhman lab,[23,40] a systematic approach to detecting MEG was unable to observe its occurrence in InAs and PbSe samples up to nearly 4 times the particle band edge energy. Given this impetus for investigating exciton cooling, an equivalent study of MEG was conducted on the sample employed here as well. As before, MEG was unobservable for these particles, and details of our failed search for MEG are provided in the Supporting Information. This result contradicts numerous recent observations of MEG in PbSe QDs, demonstrating the need for a better understanding of the processes which dominate energy relaxation of hot excitons in this system.

DISCUSSION

Spectral Signatures of Exciton Cooling. The discussion will address three novel observations described above: the instantaneous nature of the band edge bleach which we have coined $1S_B$, the unexpected kinetic correlation of A1 and A2 bands detected in the finite difference TA data, and the broad short-lived net absorption which rises between the absorption bands. All three will then be recast in terms of the difference dipole kinetics observed. Finally the independence of cooling rates on the number of excitons per quantum dot will briefly be commented on before concluding.

$1S_B$ Feature. The immediate bleach feature appearing at the band edge which is essentially unchanged in width, depth, or position during exciton cooling is inconsistent with the current understanding of hot exciton absorption in QDs. At sufficiently high photon energies, the nascent exciton should comprise an electron−hole pair, neither of which occupies its lowest-energy orbital. In previous studies of CdSe NCs an equivalent bleach was assigned as the negative part of a peak shift difference spectrum. The red-shifted positive lobe—the A1 band[6,41]—was shown to gradually decay upon exciton cooling due to fading of the biexciton shift and its replacement with a state filling bleach. This picture leads to two expectations: (a) that the negative peak shift feature could vary in its amplitude from being much weaker to exceeding the amplitude of the initial band edge absorption band and (b) that a significant spectral shift is expected upon transition to state filling.

The unchanging nature of the band edge bleach, highlighted by the zero reaching cleft in the finite difference spectra in Figure 5, can only indicate that excited QDs, regardless of exciton energy, no longer contribute to the 1S absorption band. This still will not explain the observation since biexciton interactions which modify the absorption of excited dots should affect all eight degenerate band edge transitions.[14,42] This would be consistent with photoluminescence experiments

dx.doi.org/10.1021/jp409530z | J. Phys. Chem. C 2013, 117, 26342−26350

which show that relaxed hot excitons statistically populate all four L-points in *k*-space and both spin orientations.[33,43] It is also to be expected in view of Auger recombination rate scaling with the number of excitons n_x.[44] Accordingly, if biexciton interaction drastically broadens or shifts the absorption band edge, then even a single exciton would bleach the whole 1S absorbance band regardless of the number of excitons. In contrast we find that the bleach amplitude equals $n_x/4$ times the ground state 1S absorbance right from the start—irrespective of excess photon energy. It is noteworthy that a similar decomposition of spectral bands near the band edge and their decay is hampered in CdSe due to the inherent overlap with adjacent spectral features. Testing whether the unexpected observation of a nearly instantaneous band edge bleach in hot excitons extends to the more extensively studied CdSe QDs is accordingly very difficult. Solving this riddle even in the case of PbSe will require further investigation.

Correlated A1 and A2 Peaks. As stated above, an A1-like induced absorption was observed in CdSe QDs as well and assigned to biexciton shifting of the 1S band. If indeed the assignment to biexciton shifts was applicable here, the increase in A1 amplitude with bluer pump photons must indicate that hot excitons bind more tightly. To demonstrate this effect, Sewall et al.[25] performed a simple simulation on CdSe where they increased the magnitude of the binding energy and showed how it increased the A1 absorption. While this type of modeling demonstrates an increase in the red absorption, it must also be accompanied with a proportional deepening of the matching bleach, contrary to our observations.

The only way that the bleach associated with a biexciton shift can be unchanged upon the exciton cooling to the band edge is that the state-filling feature perfectly matches the spectral shift bleach which precedes it. The possibility that such a perfect fortuitous match between the two spectra be present seems impossible. It is even more unlikely since the induced transparency component due to biexciton binding should be blue-shifted relative to the state-filling band which follows. Instead of an adjacent renewed absorption, the data indicate a perfectly correlated buildup of absorbance in the 1P band (A2), which accompanies the decay of A1.

This correlation could be explained by a shift in filling between the two lowest states but would still leave the unchanging $1S_B$ to be explained. One thing is made clear by the kinetics in Figure 6, and that is that the decay of band A1,2 is sensitive to the slowest relaxation process involved in exciton cooling since their evolution extends the longest. The induction time for the onset of their decay, which is best observed when exciting at 525 nm, is the longest, indicating that above a certain exciton energy these two features are insensitive to additional excitation. Accordingly their disappearance begins only after that same initial excess decay. It is also significant to note that once the induction period is over the tailing off of the A features follows the same exponential decay, indicating that it is dependent only on the momentary excess energy without additional memory effects. How it is that this slowest of relaxation processes has no impact on the bleach signal at the band edge is a riddle that remains unanswered. We note in passing that A2 analogs were not reported in transient spectra of hot excitons in CdSe NCs, as its observation required analysis in terms of $\Delta\Delta OD(t,\lambda)$ which was not undertaken for that material.

B and C Features. The fastest decaying features are the C and B bands, which lie between the 1S and 1P peaks in the linear absorption spectrum. Previous TA studies of PbSe QDs have reported induced absorptions in this range for hot excitons. In some cases these features have been assigned to symmetry forbidden transitions of 1P1S/1S1P, presumably due to exciton-induced symmetry breaking of the electronic structure.[24,45] In this respect it is noteworthy that of these two spectral features only the shortest lived C band matches this assignment since its width and sharpness are similar to the allowed 1S and 1P peaks. The B band in contrast is very broad and covers the range between these bands and extends even to higher frequencies.

The fact that the decay dynamics of the various bands differ so markedly could reflect different decay rates of electrons and holes—both of which can affect the transient absorption spectrum. In any case the distinct spectral and kinetic nature of the features which immediately surround the 1S bleach are incompatible with conclusions of earlier studies, which followed band edge bleach dynamics with open band pump−probe methods. In the cited studies,[6,16,22] a ∼2 ps rise component in the band edge bleach was interpreted as reflecting the transition from biexciton shifting to state filling. The cited observations might have been the result of spectral overlap of the band edge bleach with adjacent features due to spectral integration in open band detection or due to actual overlap due to broader size dispersion. These have been eliminated here by high monodispersity of the sample and hyperspectral probing of the transient absorption.

Perhaps the biggest difficulty that this interpretation poses is the virtual disappearance of the A1 band with cooling of an exciton to the band edge. This requires that for some reason a cold existing exciton does not interact at all with another band edge exciton, while mild excess energies induces very significant binding between them.[25] Taken together with the invariance of the band edge bleach with exciton cooling, and the correlation revealed between the A1 and A2 features, this observation strongly argues against the accepted view of A1 as one-half of a state shifting feature.

Difference Dipole Strength Kinetics. The kinetic analysis presented in Figure 6 allows an assignment of the spectral feature which causes the unexpected initial increase in ΔΔOD. Aside from the band edge bleach, all the other identified bands are somewhat influenced in their amplitude by the pump-photon energy. None however is nearly as dependent on the exciton excess energy as ″B″, as demonstrated by the normalized amplitudes tabulated in Table 1. This is very interesting since this transient band is also unique in its structure. Despite its appearing near the band edge, it is much broader than all other bands, including the 1S and 1P peaks in the linear spectrum.

This spectral structure is curious since interband transitions in this range, due to quantum confinement, are expected to assume the atom-like discrete nature, broadened only by the sample's inhomogeneity. One way or another the fact that the dipole strength is enhanced at early delays can have one of two explanations. One is that biexciton interactions which are specific to high-energy excitons either allow formally forbidden interband transitions or enhance others which are formally allowed.[45] The other is that we are witnessing intraband transitions which unexpectedly overlap with the interband absorption. Why the main suspect (B) is such a broad feature, why it appears in this spectral region, and whether this feature results from intra- rather than interband transitions will require further experiments. Probing this is a significant challenge since

B ranges throughout the spectral range probed in our experiments.

Single vs Multiexciton Cooling. The spectra in Figure 7 show that exciton cooling dynamics as seen by TA are the same for single and biexcitons. This insensitivity of a relaxing exciton to the presence of another is remarkable since biexciton interactions are substantial and could be envisioned to affect cooling rates by shifting energy levels or by mutually influencing the coupling to the degrees of freedom responsible for relaxation to the band edge. One such mechanism which should be drastically dependent on n_x is that of Auger cooling. As presented in the Introduction, the involvement of Auger cooling in dissipation of exciton excess energy in PbSe QDs has been debated.[17,18]

Figure 7 presents conclusive evidence that Auger cooling does not play a significant role in PbSe NCs, at least in the narrow size range we have investigated. As in the case of Auger recombination, the fact that the cooling is a two-body process means that the rate will grow at least linearly with the number of excitons since the larger the n_x, the greater the number of potential partners each electron has to transfer energy to, etc. Thus the identical rates for cooling of single and multiexcitons demonstrates the ineffectiveness of Auger cooling in this material. We note in passing that this interpretation also goes against the possibility that the kinetically distinct spectral components observed during cooling, i.e., the broad and short-lived absorption, and the two bands decaying more slowly, might represent relaxing electrons and holes or vice versa, respectively. The correct assignment of these features will require further experiments.

CONCLUSIONS

The cooling dynamics of excitons in photoexcited lead selenide quantum dots has been followed by femtosecond hyperspectral near IR probing. Spectral analysis including separation of multiexciton contributions to the data has revealed kinetically and spectrally distinct features which are incompatible with prevailing models for nanocrystal absorption and its dependence on excess energy. They appear to be at odds with the expected degeneracies of the low-lying discrete optical transitions in PbSe and exhibit kinetic correlations which defy associated energy level assignments. Transient spectra of single and double hot exciton states are similar both in appearance and in decay dynamics, arguing against the involvement of Auger cooling in the rapid exciton relaxation in PbSe QDs, and as in previous studies quantitative analysis of data collected at various pump frequencies has revealed no sign of MEG up to nearly 4 times the band gap of the current samples. All the above demonstrate that despite more than a decade of study fundamental aspects of PbSe nanocrystal spectroscopy on ultrafast time scales still remain unclear and call for further investigation.

ASSOCIATED CONTENT

Supporting Information

Band edge bleach data at high and low pump fluences are presented to demonstrate (1) that experiments can be run with high S/N where virtually no multiexcitons are generated by multiphoton absorption and (2) that by increasing the pump fluence a significant fraction of biexcitons is produced. A test for occurrence of MEG in our samples is presented demonstrating no detectable carrier multiplication up to a photon energy of nearly 4 times the band edge. Simulation of the 1P−1P band during exciton cooling is compared with TA data leading to an estimate of 20 meV for biexciton interaction in the employed sample. This material is available free of charge via the Internet at http://pubs.acs.org.

AUTHOR INFORMATION

Corresponding Author

*E-mail: sandy@mail.huji.ac.il.

Notes

The authors declare no competing financial interest.

ACKNOWLEDGMENTS

This work was supported by the James Franck program for laser matter interaction and by the Israel Science Foundation (ISF). The James Franck program is supported by the Minerva Gesellschaft, GmbH, Munich, Germany. The ISF is administered by the Israel Academy of Sciences and the Humanities.

REFERENCES

(1) Murray, C. B.; Kagan, C. R.; Bawendi, M. G. Synthesis and Characterization Of Monodisperse Nanocrystals and Close-Packed Nanocrystal Assemblies. *Annu. Rev. Mater. Sci.* **2000**, *30*, 545−610.

(2) Bockelmann, U.; Bastard, G. Phonon Scattering and Energy Relaxation in Two-, One-, and Zero-Dimensional Electron Gases. *Phys. Rev. B* **1990**, *42* (19), 8947−8951.

(3) Nozik, A. Quantum Dot Solar Cells. *Phys. E* **2002**, *14*, 115−120.

(4) Semonin, O. E.; Luther, J. M.; Choi, S.; Chen, H.-Y.; Gao, J.; Nozik, A. J.; Beard, M. C. Peak External Photocurrent Quantum Efficiency Exceeding 100% via MEG in a Quantum Dot Solar Cell. *Science* **2011**, *334* (6062), 1530−1533.

(5) Wehrenberg, B. L.; Wang, C.; Guyot-Sionnest, P. Interband and Intraband Optical Studies of PbSe Colloidal Quantum Dots. *J. Phys. Chem. B* **2002**, *106* (41), 10634−10640.

(6) Klimov, V. I. Optical Nonlinearities and Ultrafast Carrier Dynamics in Semiconductor Nanocrystals. *J. Phys. Chem. B* **2000**, *104* (26), 6112−6123.

(7) Cooney, R. R.; Sewall, S. L.; Anderson, K. E.; Dias, E. A.; Kambhampati, P. Breaking the Phonon Bottleneck for Holes in Semiconductor Quantum Dots. *Phys. Rev. Lett.* **2007**, *98* (17), 177403.

(8) Efros, A. L.; Kharchenko, V. A.; Rosen, M. Breaking the Phonon Bottleneck in Nanometer Quantum Dots: Role of Auger-Like Processes. *Solid State Commun.* **1995**, *93* (4), 281−284.

(9) Wang, L. W.; Califano, M.; Zunger, A.; Franceschetti, A. Pseudopotential Theory of Auger Processes in CdSe Quantum Dots. *Phys. Rev. Lett.* **2003**, *91* (5), 564041−564044.

(10) Guyot-Sionnest, P.; Shim, M.; Matranga, C.; Hines, M. Intraband Relaxation in CdSe Quantum Dots. *Phys. Rev. B* **1999**, *60* (4), 2181−2184.

(11) Hendry, E.; Koeberg, M.; Wang, F.; Zhang, H.; de Mello Donegá, C.; Vanmaekelbergh, D.; Bonn, M. Direct observation of electron-to-hole energy transfer in CdSe quantum dots. *Phys. Rev. Lett.* **2006**, *96* (5), 0574088.

(12) Xu, S.; Mikhailovsky, A. A.; Hollingsworth, J. A.; Klimov, V. I. Hole Intraband Relaxation in Strongly Confined Quantum Dots: Revisiting the "Phonon Bottleneck" Problem. *Phys. Rev. B* **2002**, *65* (4), 045319.

(13) Vaxenburg, R.; Lifshitz, E. Alloy and heterostructure architectures as promising tools for controlling electronic properties of semiconductor quantum dots. *Phys. Rev. B* **2012**, *85* (7), 075304.

(14) Inuk, K.; Wise, F. W. Electronic Structure and Optical Properties of PbS and PbSe Quantum Dots. *J. Opt. Soc. Am. B* **1997**, *14*, 1632−1646.

(15) Wehrenberg, B. L.; Wang, C.; Guyot-Sionnest, P. Interband and Intraband Optical Studies of PbSe Colloidal Quantum Dots. *J. Phys. Chem. B* **2002**, *106*, 10634.

(16) Harbold, J.; Du, H.; Krauss, T.; Cho, K.-S.; Murray, C.; Wise, F. Time-resolved Intraband Relaxation of Strongly Confined Electrons

and Holes in Colloidal PbSe Nanocrystals. *Phys. Rev. B* **2005**, *72*, 195312.
(17) Schaller, R. D.; Pietryga, J. M.; Goupalov, S. V.; Petruska, M. A.; Ivanov, S. A.; Klimov, V. I. Breaking the Phonon Bottleneck in Semiconductor Nanocrystals via Multiphonon Emission Induced by Intrinsic Nonadiabatic Interactions. *Phys. Rev. Lett.* **2005**, *95* (19), 196401.
(18) An, J. M.; Franceschetti, A.; Dudiy, S. V.; Zunger, A. The Peculiar Electronic Structure of PbSe Quantum Dots. *Nano Lett.* **2006**, *6* (12), 2728−2735.
(19) An, J. M.; Califano, M.; Franceschetti, A.; Zunger, A. Excited-State Relaxation in Pbse Quantum Dots. *J. Chem. Phys.* **2008**, *128*, 164720.
(20) Klimov, V. I. Spectral and Dynamical Properties of Multiexcitons in Semiconductor Nanocrystals. *Annu. Rev. Phys. Chem.* **2007**, *58*, 635−673.
(21) Kambhampati, P. Hot Exciton Relaxation Dynamics in Semiconductor Quantum Dots: Radiationless Transitions on the Nanoscale. *J. Phys. Chem. C* **2011**, *115*, 22089−22109.
(22) Klimov, V. I.; McBranch, D. W. Femtosecond 1P-to-1S Electron Relaxation in Strongly Confined Semiconductor Nanocrystals. *Phys. Rev. Lett.* **1998**, *80* (18), 4028−4031.
(23) Gdor, I.; Sachs, H.; Roitblat, A.; Strasfeld, D. B.; Bawendi, M. G.; Ruhman, S. Exploring Exciton Relaxation and Multiexciton Generation in PbSe Nanocrystals Using Hyperspectral Near-IR Probing. *ACS Nano* **2012**, *6* (4), 3269−3277.
(24) Schins, J. M.; Trinh, M. T.; Houtepen, A. J.; Siebbeles, L. D. Probing Formally Forbidden Optical Transitions in PbSe Nanocrystals by Time-and Energy-Resolved Transient Absorption Spectroscopy. *Phys. Rev. B* **2009**, *80* (3), 035323.
(25) Sewall, S. L.; Cooney, R. R.; Dias, E. A.; Tyagi, P. Kambhampati State-Resolved Observation in Real Time of the Structural Dynamics of Multiexcitons in Semiconductor Nanocrystals. P. *Phys. Rev. B* **2011**, *84* (23), 235304.
(26) Gesuele, F.; Sfeir, M.; Koh, W.; Murray, C. B.; Heinz, T. F.; Wei Wong, C. Ultrafast Supercontinuum Spectroscopy of Carrier Multiplication and Biexcitonic Effects in Excited States of PbS Quantum Dots. *Nano Lett.* **2012**, *12* (6), 2658−2664.
(27) Wand, A.; Rozin, R.; Eliash, T.; Jung, K. H.; Sheves, M.; Ruhman, S. Symmetric Toggling of a Natural Photoswitch: Ultrafast Spectroscopy of Anabaena Sensory Rhodopsin. *J. Am. Chem. Soc.* **2011**, *133* (51), 20922−20932.
(28) Liljeroth, P.; van Emmichoven, P. A. Z.; Hickey, S. G.; Weller, H.; Grandidier, B.; Allan, G.; Vanmaekelbergh, D. Density of States Measured by Scanning-Tunneling Spectroscopy Sheds New Light on the Optical Transitions in PbSe Nanocrystals. *Phys. Rev. Lett.* **2005**, *95* (8), 086801.
(29) Trinh, M. T.; Houtepen, A. J.; Schins, J. M.; Piris, J.; Siebbeles, L. D. A. Nature of the Second Optical Transition in PbSe Nanocrystals. *Nano Lett.* **2008**, *8* (7), 2112−2117.
(30) Peterson, J. J.; Huang, L.; Delerue, C.; Allan, G.; Krauss, T. D. Uncovering Forbidden Optical Transitions in PbSe Nanocrystals. *Nano Lett.* **2007**, *7* (12), 3827−3831.
(31) Sewall, S.; Franceschetti, A.; Cooney, R.; Zunger, A.; Kambhampati, P. Direct Observation of the Structure of Band-edge Biexcitons in Colloidal Semiconductor CdSe Quantum Dots. *Phys. Rev. B* **2009**, *80*, 081310.
(32) Knox, R. S. Dipole and Oscillator Strengths of Chromophores in Solution. *Photochem. Photobiol.* **2007**, *77*, 492−496.
(33) McGuire, J. A.; Joo, J.; Pietryga, J. M.; Schaller, R. D.; Klimov, V. I. New Aspects of Carrier Multiplication in Semiconductor Nanocrystals. *Acc. Chem. Res.* **2008**, *41* (12), 1810−1819.
(34) Ellingson, R. J.; Beard, M. C.; Johnson, J. C.; Yu, P.; Micic, O. I.; Nozik, A. J.; Shabaev, A.; Efros, A. L. Highly Efficient Multiple Exciton Generation in Colloidal PbSe and PbS Quantum Dots. *Nano Lett.* **2005**, *5*, 865−871.
(35) Sukhovatkin, V.; Hinds, S.; Brzozowski, L.; Sargent, E. H. Colloidal Quantum-Dot Photodetectors Exploiting Multiexciton Generation. *Science* **2009**, *324* (5934), 1542−1544.
(36) Xiao, J.; Wang, Y.; Hua, Z.; Wang, X.; Zhang, C.; Xiao, M. Carrier Multiplication in Semiconductor Nanocrystals Detected by Energy Transfer to Organic Dye Molecules. *Nat. Commun.* **2012**, *3*, 1170.
(37) Stubbs, S. K.; Hardman, S. J. O.; Graham, D. M.; Spencer, B. F.; Flavell, W. R.; Glarvey, P.; Masala, O.; Pickett, N. L.; Binks, D. J. Efficient Carrier Multiplication in InP Nanoparticles. *Phys. Rev. B* **2010**, *81*, 081303.
(38) Ji, M.; Park, S.; Connor, S. T.; Mokari, T.; Cui, Y.; Gaffney, K. J. Efficient Multiple Exciton Generation Observed in Colloidal PbSe Quantum Dots with Temporally and Spectrally Resolved Intraband Excitation. *Nano Lett.* **2009**, *9*, 1217−1222.
(39) Yang, Y.; Rodríguez-Córdoba, W.; Lian, T. Multiple Exciton Generation and Dissociation in PbS Quantum Dot-Electron Acceptor Complexes. *Nano Lett.* **2012**, *12*, 4235−4241.
(40) Ben-Lulu, M.; Mocatta, D.; Bonn, M.; Banin, U.; Ruhman, S. On the Absence of Detectable Carrier Multiplication In A Transient Absorption Study of InAs/CdSe/ZnSe Core/Shell1/Shell2 Quantum Dots. *Nano Lett.* **2008**, *8* (4), 1207−1211.
(41) Kambhampati, P. Unraveling the Structure and Dynamics of Excitons in Semiconductor Quantum Dots. *Acc. Chem. Res.* **2011**, *44* (1), 1−13.
(42) Kang, I.; Wise, F. W. Electronic Structure and Optical Properties of PbS and PbSe Quantum Dots. *J. Opt. Soc. Am. B* **1997**, *14*, 1632.
(43) Nair, G.; Geyer, S.; Chang, L.-Y.; Bawendi, M. Carrier Multiplication Yields in PbS and PbSe Nanocrystals Measured by Transient Photoluminescence. *Phys. Rev. B* **2008**, *78*, 125325.
(44) Klimov, V.; McGuire, J.; Schaller, R.; Rupasov, V. Scaling of Multiexciton Lifetimes in Semiconductor Nanocrystals. *Phys. Rev. B* **2008**, *77*, 195324.
(45) Burda, C.; Link, S.; Green, T. C.; El-Sayed, M. A. New Transient Absorption Observed in the Spectrum of Colloidal CdSe Nanoparticles Pumped with High-Power Femtosecond Pulses. *J. Phys. Chem. B* **1999**, *103*, 10775−10780.